



From Changing Environment to Changing Extremes: Exploring the Future Streamflow and Associated Uncertainties Through Integrated Modelling System

Srishti Gaur¹ · Arnab Bandyopadhyay² · Rajendra Singh¹

Received: 4 December 2020 / Accepted: 21 March 2021 / Published online: 15 April 2021
© The Author(s), under exclusive licence to Springer Nature B.V. 2021

Abstract

Climate and land-use changes can alter the dynamics of hydro-climatic extremes by modifying the flow regimes. Here, we have attempted to disentangle the relationship between changing environmental conditions and hydro-climatic extremes considering associated uncertainties for the Subarnarekha, a flood prone-basin of India. A comprehensive, integrated modelling system was developed that incorporates a spatially explicit land-use model, a hydrological model, and an ensemble of regional climate models (RCMs). MIKE SHE/MIKE HYDRO RIVER was used to simulate the hydrological processes. The uncertainties associated with model parameters, model inputs, and model structures are analysed collectively using ‘quantile regression.’ A transferable framework was developed for the analysis of hydro-climatic extremes that deal with numerous aspects like sensitivity, occurrences, severity, and persistence for four-time horizons: baseline (1976–2005) and early (2020s), mid (2050s), end-centuries (2080s). ANOVA is used for partitioning uncertainty due to different sources. The results obtained from numerous analysis of the developed framework suggests that low, high, and medium flows will probably increase in the future (20%-85% increase), indicating a higher risk of floods, especially in the 2050s and 2080s. Partitioning of uncertainty suggests RCMs contribute 40%-62% to the uncertainty in streamflow projections. The developed modelling systems incorporates a flexible framework so update any other water sustainability issue in the future. These findings will help better meet the challenges associated with the possible risk of increasing high flows in the future by ceding references to the decision-makers for framing better prevention measures associated with land-use and climate changes.

Keywords ANOVA · Climate change · Land-use change · MIKE SHE · MIKE HYDRO RIVER · Quantile regression · Transferable methodology · Uncertainty

✉ Srishti Gaur
srishtigaur76@gmail.com

Extended author information available on the last page of the article

1 Introduction

Land and water resources are the two intricate systems existing on the planet that is often taken for granted by humanity (Wijesekara 2013). From a hydrological perspective, rapidly changing climate and continuous evolution in land use and land cover (LULC) are prominent factors that are thoroughly intertwined for pressurising these systems (Goyal and Surampalli 2018). Moreover, over-exploitation of land and water resources at various spatial and temporal scales has far-reaching implications on the environment, economy, and society. Therefore, these systems must be understood and managed as coherent dynamic entities to warrant their integrity.

In light of the above, the combined investigation of climate and LULC changes is essential to ensure land and water resources for the upcoming generations. The most deteriorating extreme impacts of climate and LULC change are the increasing dichotomy of drought and floods. Specifically, the most worrisome trend is no rain for a longer duration followed by sudden bout in rainfall intensities, causing flash floods, which leads to substantial revenue losses. Hence, understanding the dynamics of hydro-climatic extremes along with climate and LULC change holds tremendous interest.

In the recent past, numerous studies have focused on the isolated impacts of LULC and climate change; however, relatively fewer studies have considered the combined changes in projecting future water availability. The prime concern of these studies is to predict the streamflow as it has a vital role in water resources management and planning (Kim et al. 2020; Mohammadi et al. 2020a, b). Furthermore, integrated modelling systems are desirable to unravel the dynamics of such changes to understand the hydrological process. Such systems considered so far in the literature have limitations in addressing the complexity of major physical processes. In this regard, a physically-based, fully distributed hydrological model generates potentially more precise results than a model operated at a lumped scale (Farjad et al. 2017).

Consideration of uncertainty framework in the hydrological impact analysis is essential for the quantifying future water availability (Beven and Feyen 2002; Tabari 2015; Norouzi Khatiri et al. 2020; Anaraki et al. 2021). Projecting hydrological responses of combined climate and LULC changes is usually subjected to substantial uncertainties. These uncertainties may be due to representative concentration pathways (RCPs), climatic projections by general circulation models (GCMs)/regional climate models (RCMs), internal variability of hydrological processes, and hydrological model, and may get propagated through complex modelling chain (Pechlivanidis et al. 2017). The sources mentioned, however, do not contribute equally to the total uncertainty in streamflow projections. Therefore, it is essential to segregate the contribution of each uncertainty source to the total uncertainty. Furthermore, the uncertainty in model inputs and model parameters also propagated to modelling outcomes (Kundzewicz et al. 2018).

The analysis of hydro-climatic extremes performed through the combination of climate and hydrological models often lag in terms of well-defined methodologies. Key research activities of such studies are limited to the analysis of historical trends in hydro-meteorological variables and the projection of future hydrological states. Gaur et al. (2020a) studied the impacts of climate change on the Subarnarekha basin. However, the study has several limitations, e.g., only isolated impacts of climate change were considered without considering LULC changes, appropriate selection of ensemble members and uncertainty associated with selecting a hydrological model. Accordingly, more study is needed to deal with systematic methodologies for analysis and prediction of hydro-climatic extremes. The present study addresses this research gap and contributes to the comprehensive understanding of the projection of hydro-climatic

extremes under changing environmental conditions while considering the associated uncertainties for the Subarnarekha basin.

Subarnarekha is abundant in natural resources. However, anthropogenic activities like deforestation, urbanisation, large-scale mining, and industrialisation, in combination with climate change, have significantly impacted the hydrological processes in the basin. These consequences have resulted in severe soil degradation in the upper catchments and increasing susceptibility to flash floods (Singh and Giri 2018).

We have used an integrated modelling system (details in Sect. 2.3) that consists of a unique combination of MIKE SHE/MIKE HYDRO, Multilayer-perceptron Markov model (MLP-M) and an ensemble of RCMs to simulate the combined surface water and groundwater interaction in the basin. Here, we have incorporated the changes in the land surface's physical properties in the simulation of future hydrological processes. All kinds of model uncertainties are answered through Quantile Regression. The segregation of uncertainty due to each source is performed through ANOVA.

The study attempts to develop a novel transferable methodology that helps develop a better understanding of hydro-climatic extremes' prediction through the integrated modelling system. The developed framework may also capture sensitivities of streamflows towards changing variability, relative stabilities of future streamflows with respect to the baseline period (i.e., dispersivity) and shifting in timing (date of occurrence) and uniformity (persistence) of extreme events. To investigate further whether floods (or droughts) over Subarnarekha will be more frequent in the future, we have formulated the following set of research questions to be answered through the framework:

1. What will be the trends and abrupt changes in extreme flow across Subarnarekha during the 2020s, 2050s, and 2080s?
2. How will the Subarnarekha basins' sensitivity towards climate change vary during the 2020s, 2050s, and 2080s?
3. How will the stability of future streamflow vary during the 2020s, 2050s, and 2080s with respect to the baseline period?
4. Will there be any shift in the occurrence and persistence of extreme events during the 2020s, 2050s, and 2080s with respect to the baseline period?
5. What will be the significant contributing sources to uncertainty in streamflow projections in the basin?

The novelty of the study lies in developing a comprehensive, integrating modelling system that combines the land-use, hydrology and regional climate models, and leads to developing a transferable methodology to better understand the dynamics of hydro-climatic extremes under changing environment.

The developed integrated modelling system will better understand the past, ongoing, and future climate and land-use changes that may help the environmentalists, hydrologists, and policymakers in water management and better policy intervention.

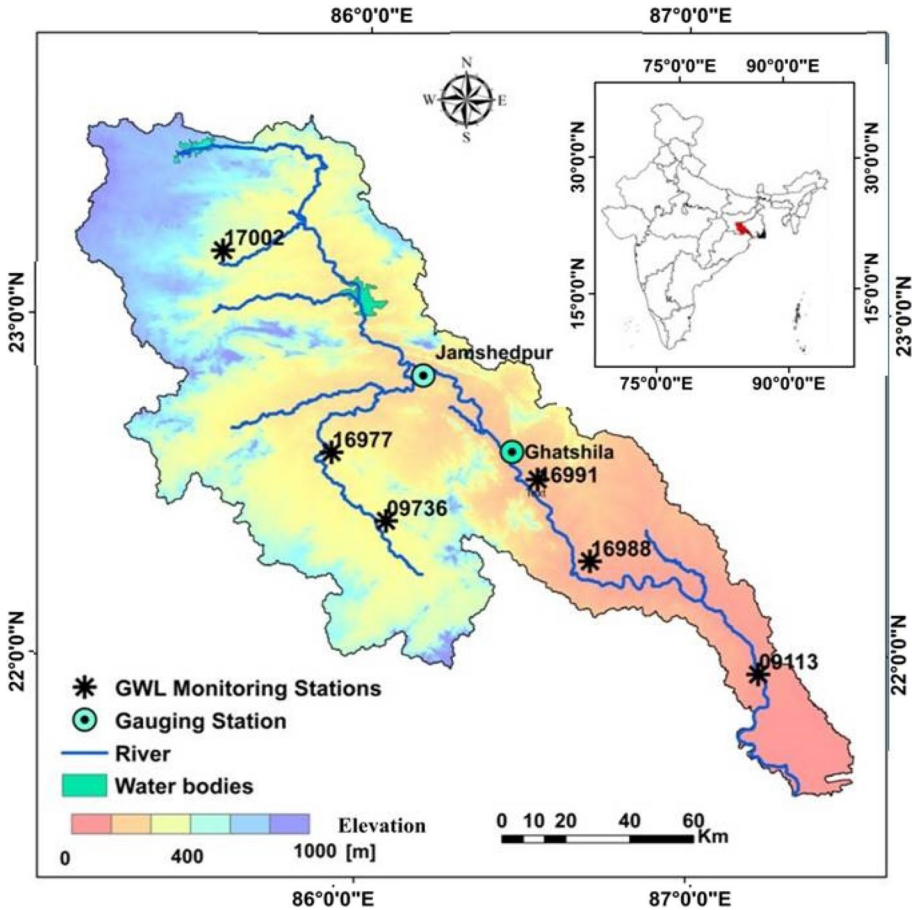


Fig. 1 Index map of Subarnarekha river basin

2 Method

2.1 Study Area

The Subarnarekha basin (Fig. 1) passes through three Indian states Jharkhand, Odisha, and West Bengal, and drains a catchment area of 19,296 km² spanning over 450 km. The climate of the basin is tropical, with a mean annual rainfall of 1800 mm (Paul et al. 2019). Subarnarekha receives 82% of the flow from the southwest monsoon from June to September. The average temperature of the basin varies from 9 °C to 42 °C. The basin is flood-prone and characterised by a complex hydrological regime owing to variations in climate, geomorphology, and topography, thus, making it an interesting study to pursue.

Two major reservoirs, Chandil and Getalshud, are situated inside the basin (Fig. 1). In the present study, two gauging stations, i.e., Jamshedpur and Ghatshila, and six groundwater monitoring stations (17,002, 16,977, 09,736, 16,991, 16,988, and 09,113) are considered to calibrate the surface water and groundwater interaction.

Figure 1 presents the locations of the gauging stations and the groundwater level (GWL) monitoring stations. Figure S1 in supplementary material presents the area drained by the gauging stations.

2.2 Data

The climatic variables required in MIKE SHE/MIKE HYDRO RIVER are precipitation, maximum and minimum temperature, and potential evapotranspiration. Among them, precipitation and maximum and minimum temperature datasets are taken from India Meteorological Department (IMD), Pune at $0.25^\circ \times 0.25^\circ$ and $1^\circ \times 1^\circ$ resolutions, respectively. The potential evapotranspiration is estimated using the Hargreaves method (Hargreaves and Samani 1985). Observed discharge data is taken from the Central Water Commission (CWC), Bhubaneswar. The observed data for GW monitoring wells, at the seasonal scale, are taken from the Central Ground Water Board (CGWB).

The LULC maps of the basin are prepared using Landsat TM and Landsat ETM imagery of 1989, 1994, 2006, and 2011 by applying the unsupervised classification. The major LULC classes are water bodies, dense forest, scrubland, barren land, and built-up area. The predicted LULC maps (2020, 2030, and 2040) by MLP-M Model are obtained from Gaur et al. (2020b). Figure S2 presents the statistics of the distribution of each LULC class during 1989–2011. The model details and the utilised explanatory variables can be accessed from Gaur et al. (2020b).

The future simulations are carried out using the data from CORDEX-South Asia for all available RCMs (i.e., 19 RCMs) for 1976–2005 (baseline period, from now on), 2010–2039 (the 2020s, from now on), 2040–2069 (2050s, from now on), and 2070–2099 (2080s, from now on) under two RCPs, RCP4.5 and RCP8.5. Here, the ensemble means for projected climate variables (rainfall and maximum and minimum temperature) are generated using SCM as it outperforms the other two ensemble techniques (Random Forest and Support Vector Regression as per Singh, (2019)). The selection of the most appropriate sub-ensemble members (i.e., RCMs) is performed based on their ability to mimic their respective observed dataset's spatial patterns through spatial performance metrics as suggested in Singh (2019) during the baseline period. Climate data is bias-corrected using 'quantile mapping' (Piani et al. 2010).

Being a physically-based model, MIKE SHE/MIKE HYDRO RIVER requires an intensive amount of data. The details of the datasets required for setting up the MIKE SHE/MIKE HYDRO RIVER model are presented in Table S1.

2.3 Integrated Modelling Technique

An integrated modelling system is formed by combining i) MIKE SHE/MIKE HYDRO RIVER model; ii) MLP-M, spatial-explicit LULC model; iii) Ensemble projections of most suitable RCMs for Subarnarekha basin, and iv) a flexible framework in which any new plan related to water sustainability can be easily incorporated in future.

Hydrologic model MIKE SHE along with river model MIKE HYDRO RIVER is a comprehensive, physically-based, and distributed modelling system that is capable of simulating almost all processes of the land phase of the hydrological cycle.

MIKE SHE provides numerous approaches, ranging from simple, lumped, conceptual to advanced, distributed, and physically-based (Wijesekara et al. 2012). An advanced, fully distributed version is utilised here, considering the surface and sub-surface water

Table 1 Performance evaluation measures during streamflow simulation

		NSE	R ²	Ln(NSE)	RMSE (m ³ /s)	PBIAS (%)	SD (m ³ /s)
Jamshedpur	Calibration	0.78	0.82	0.68	188.30	-22	398
	Validation	0.72	0.78	0.63	265.30	-23	540
Ghatshila	Calibration	0.81	0.82	0.61	240.6	-10	404
	Validation	0.74	0.84	0.67	192	-24	592

components (overland flow, channel flow, and saturated zone flow) as governing components to fulfil the purpose of the study. The boundary of the catchment was delineated using a 30 m DEM (Table 1). The model domain was discretised in 500 m grid size. The climate data (i.e., precipitation and maximum and minimum temperatures) are interpolated to 500 m using bi-linear interpolation. Similarly, the spatial maps of other datasets (topography maps, LULC maps, roughness coefficients, detention storage, soil maps, horizontal hydraulic conductivity, vertical hydraulic conductivity, specific yield, specific storage, and initial potential head) are interpolated to 500 m and given as input to the model in fully distributed form. Table S2 in supplementary material presents the details of the methods used in the present study to simulate the dominant hydrological processes.

A 1-D hydrodynamic model, MIKE HYDRO RIVER, was used to simulate the channel flow. The river network was generated using ArcGIS. It consists of six branches and two reservoirs. The upstream boundary of the river was set to ‘closed’ (i.e., no-flow boundaries), and the downstream boundary condition was selected by ‘flow versus water level (Q-H boundary)’.

2.4 Description of Methodology

2.4.1 Performance Evaluation of MIKE SHE/MIKE HYDRO RIVER Model

For the comprehensive evaluation of the streamflow simulation against the observed streamflow, the dimensionless measures, i.e., Nash–Sutcliffe efficiency (NSE), coefficient of determination (R²), logarithmic NSE ((Ln) NSE), the error-index, i.e., Percent bias (PBIAS), and the dimensional measure, i.e., root mean square error (RMSE) are used. The rationale behind incorporating Ln (NSE) is NSE’s insensitivity to model over/under prediction, especially for low flows (Wijesekara 2013). In such a case, Ln (NSE) offers an increase in low flow values by flattening the peak discharge values and simultaneously keeping the high flow values intact.

For evaluating the groundwater level simulations, coefficient of determination (R²) and root mean square error (RMSE) is used. The details of the evaluation measures and their corresponding ranges are presented in Appendix A1.

2.4.2 Uncertainty Analysis Due to Hydrological Impact Model

A stochastic approach, the ‘quantile regression (QR)’ technique, is used to analyse the uncertainties arising from all sources (model inputs, model parameters, and model structure) in the streamflow and the GW levels (Weerts et al. 2011). In QR, the observed, simulated, and residual values of the respective streamflow/GW levels are associated by:

$$Q(t) = \hat{Q}(t) + r(t) \quad (1)$$

$$H(t) = \hat{H}(t) + r(t) \quad (2)$$

Where $Q(t)$ and $H(t)$ are observed streamflow and groundwater levels, $\hat{Q}(t)$ and $\hat{H}(t)$ are simulated streamflow and groundwater levels, and $r(t)$ are the residuals.

QR holds a functional relationship among the residuals and estimates in Gaussian domain, i.e., NQR (Normalised quantile regression) and NQD/NQH (Normalised quantile discharge/head) (Kumar et al. 2015), and is expressed as:

$$NQR = a \times NQD + b \quad (3)$$

$$NQR = a \times NQH + b \quad (4)$$

Distinct QR lines are obtained by minimising the absolute bias by allocating different weights to (+)ve and (-)ve residuals in the Gaussian domain. In this instance, absolute bias is considered as objective function as follows:

$$\text{Minimize } \sum \rho_{\tau}(NQR - (a \times NQD + b)) \quad (5)$$

$$\text{Minimize } \sum \rho_{\tau}(NQR - (a \times NQH + b)) \quad (6)$$

Where ρ_{τ} is the regression function responsible for placing the regressing line at the desired location, a is the slope, and b is the intercept of the regression line.

For estimating the streamflow/head, the simulated streamflow/head is first converted to the Gaussian domain as NQD; subsequently, the error in the Gaussian domain, NQR, is assessed using the regression line (i.e., using Eqs. 3–4). The assessed error, NQR, is converted to the original domain using the pre-estimated mean and standard deviation of the residual. As a final step, the estimated residual is added to daily simulated streamflow to obtain the streamflow, including uncertainty. Regression lines are used to analyse uncertainty in the simulated streamflow for different confidence intervals (CIs). Equations (5–6) estimate the slope and intercept of these lines using the calibration period data. Likewise, to validate the correctness of error models, the same model is applied for both calibration and validation periods for streamflow/head.

2.4.3 Simulating the Impact of Combined Land-Use Change and Climate Change

A critical limitation associated with LULC projections is its applicability for short term projection, i.e., typically for one-two decades (Serneels et al. 2001). Here, LULC projections are considered until 2040 in the present work. Therefore, in the combined LULC and climate change analyses of the hydrological process, the LULC scenarios are nonstationary until 2040. Afterwards, only climate change is considered.

The simulated LULC maps (1989, 1994, 2006, 2011, 2020, 2030, and 2040) are used to extract the LULC-based parameters for each LULC class. The maps include spatially distributed maps of Manning's M (surface roughness), detention storage, paved runoff coefficient, and overland groundwater leakage coefficient. The spatially distributed time series for vegetation properties (i.e., LAI and RD) are prepared as per the distribution of each LULC class in the LULC map. The ensemble climate projections (precipitation) for the 2020s, 2050s, and 2080s under two RCP scenarios, RCP4.5 and RCP8.5, are taken from Singh (2019). Similarly, the ensemble projections for minimum and maximum temperatures are used to generate potential evapotranspiration.

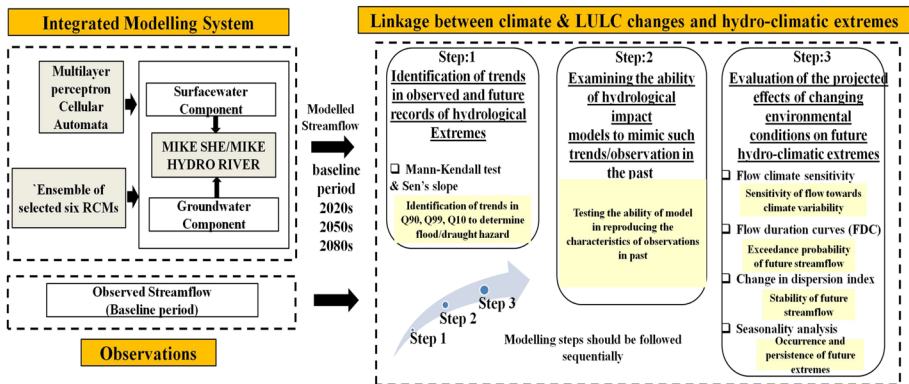


Fig. 2 Details of the generalised framework

2.4.4 Understanding of Linkage Between the Combined LULC and Climate Change and Hydro-Climatic Extremes

Here, we have attempted to develop a step-wise transferrable methodology to assess the possible linkage between the combined LULC and CC and hydro-climatic extremes motivated by Dodson et al. (2020). Figure 2 presents the details of methodology.

Step 1: Identification of trends in observed and future records of hydrological extremes

The first step to assess the existence of hydro-climatic extremes is the identification of trends. Analysis of trends is considered the fundamental process to assess the climate of a region. If the trends are significant for a variable in the region, it reflects strong climate change possibilities. The trend estimation is performed by assuming the null hypothesis that there is no trend in the hydrological series at a given significance level. A positive/negative trend in high flows suggests an increase/reduction in flood hazards, whereas a negative/positive trend in low flow suggests an increase/reduction in drought hazard (Pechlivanidis et al. 2017).

The Mann–Kendall test (Mann 1945; Kendall 1975) is a well-recognised method for estimating trends; however, the existence of autocorrelations in the time-series could increase the significant number of false positives outcomes (Storch et al. 1999). Hence, nonparametric Mann–Kendall test, with corrections for ties and auto-correlation (Hamed and Ramachandra Rao 1998), is used for estimating trends in the annual series of Q_{10} (90th exceedance percentile, high flow), Q_{01} (99th exceedance percentile, very high flow), and Q_{90} (10th exceedance percentile, low flow) during the baseline period, the 2020s, 2050s, and 2080s. If a trend is present in the data, then the slope (change per unit time) is estimated using a nonparametric procedure (Sen 1968).

Step 2: Examining the ability of hydrological impact models to mimic such trends/observation in the past

The second step includes attribution of estimated trends to historical climate change, e.g., if there are positive trends in the hydrological extremes, then whether the hydrological impact model could capture the hydro-climatic extremes in the baseline period? This step assures the credibility of the impact model in mimicking the observations in the past.

Step 3: Evaluation of the projected effects of changing environmental conditions on future hydro-climatic extremes

After testing the suitability of the hydrological model, the third step deals with finding the answer to science questions: Do the projected environmental conditions lead to intensifying/diminishing future hydro-climatic extremes?

• Streamflow climate sensitivity

The streamflow climate sensitivity determines the sensitivity of the river streamflow to climate variability. It deals with the inspection of the sensitivities of Q_{90} (low flow) and Q_{10} (high flow) to P_{mean} (mean precipitation). The analysis involves estimating the relative changes in Q_{90} , Q_{10} , and P_{mean} during 2010–2099 with respect to the baseline period and then analysing the respective $Q_{90}(Q_{10})$ versus P_{mean} relationship.

• Flow duration curves (FDC)

FDC analysis helps determine the percentage of time the river flow exceeds/falls below a particular value known to cause flood/drought damage. Projected streamflows are compared with the observed ones through the FDCs for high, medium, and low flows.

• Change in dispersion coefficient

Change in dispersion coefficient determines the stability of streamflows during the 2020s, 2050s, 2080s with respect to the baseline period. Dispersion coefficient (in %) is calculated as $\frac{(Q_{25}-Q_{75})}{Q_{50}} \times 100$, i.e., the 75th exceedance percentile flow minus the 25th exceedance percentile flow divided by the 50th exceedance percentile flow (Zhang et al. 2016). Change in dispersion coefficient is determined by calculating it for the future periods with respect to the baseline period.

• Seasonality analysis

Seasonality analysis is performed to estimate the persistence and occurrences of peak discharge events (PDE) through circular statistics. Seasonality analysis is performed in terms of seasonality index (SI) (Laaha and Bloschl 2006). The details of SI can be obtained from Appendix A2.

2.4.5 Segregation of Uncertainty Due to Different Sources

The segregation of uncertainty due to RCMs, RCPs, the interaction between RCM and RCP, and internal variability is performed using ANOVA. The details of the ANOVA model used for the disintegration of uncertainty are given in Appendix A2.

Unlike the other methodologies (Lee et al. 2017; Kim et al. 2019), ANOVA has a unique feature, i.e., quantifying the uncertainty due to the interaction term. Consideration of the interaction term is equally vital as ignoring this term could impact the data interpretation (Kim et al. 2019).

3 Results

3.1 Calibration and Validation of MIKE SHE/MIKE HYDRO RIVER Model

Model calibration and validation were performed against streamflow and groundwater levels using ten-years (1997–2006) and seven-year (2007–2013) daily records for calibration and validation. The model used 1996 as a warm-up period. At the commencement of the study, the observed streamflow and GW level data were available only until 2013. The parameters used for calibration of the surface water model are vegetation parameters (LAI and root depth), Manning's number, detention storage, initial water depth, soil parameters (water content at saturation, water content at field capacity, water content at the wilting point, saturated hydraulic conductivity), and evapotranspiration coefficients (C_1 , C_2 , and C_3). The groundwater model parameters used for calibration are horizontal and vertical hydraulic conductivities, specific retention, and specific storage.

3.1.1 Calibration and Validation Against Streamflow

Model calibration and validation against streamflow were performed at Jamshedpur and Ghatshila stations. A sensitivity analysis was performed before the calibration, which suggested surface roughness coefficient (LULC-wise Manning's M), saturated hydraulic conductivity of soils in the study area (K_{sat}), evapotranspiration coefficients (C_1 , C_2 , and C_3), and the horizontal and vertical hydraulic conductivities of the aquifer material (K_h and K_v) as the sensitive parameters.

Figures 3(a)–(h) present the time series plots along with the scatter plots for corresponding observed and simulated streamflows during calibration/validation at Jamshedpur and Ghatshila stations, respectively. It is evident from Fig. 3 that MIKE SHE/MIKE HYDRO RIVER effectively captures the temporal patterns and overall trends of the observed streamflow during both calibration and validation periods at both stations. Table 1 presents the performance evaluation measures obtained during the calibration/validation of the model at Jamshedpur and Ghatshila stations.

As modelling extremes is the main focus of the present work, capturing peak and low flows simultaneously is deemed a primary concern. Peaks are effectively captured, in general, except at a few points during calibration periods at both stations (Fig. 3). The magnitudes of $\text{Ln}(\text{NSE})$ (Table 2) suggest that the model effectively captures low flows.

Overall, as per the criteria suggested by Moriasi et al. (2007), model performance is good in simulating the streamflow. Furthermore, the model can capture the patterns of high-flows, the medium flows, and low flows reasonably well (i.e., justified by the magnitude of NSE and $\text{Ln}(\text{NSE})$). The PBIAS values (Table 2) are found to be overestimated by the model; nonetheless, its magnitude lies within the optimum limits ($-25\% < \text{PBIAS} < 25\%$). The criteria for RMSE (given in Appendix A) suggest accurate RMSE values.

3.1.2 Calibration and Validation Against Groundwater Levels

Figures 4(a)–(f) present the time series plots for calibration/validation at selected GWL stations. Table 2 presents the statistical indicator at selected GWL stations. It is evident from Table 2 that, as per Moriasi et al. (2007), the model performs reasonably well for all wells.

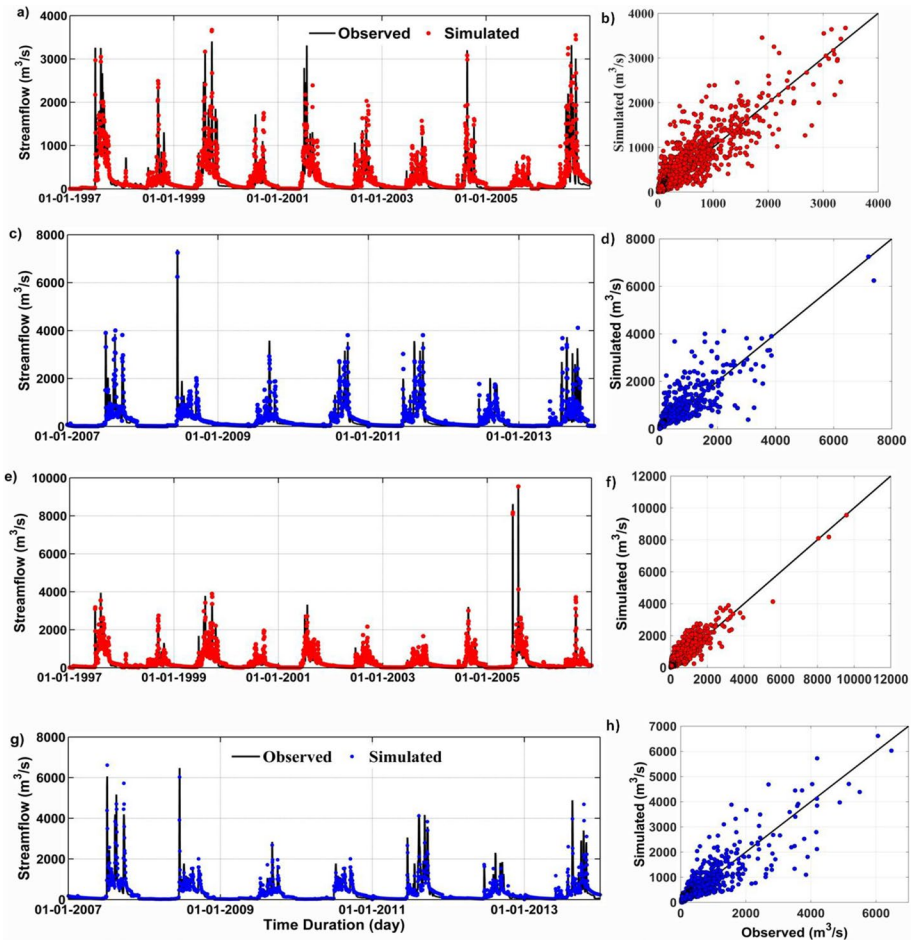


Fig. 3 Testing of hydrological model against streamflow: (a-d) Time-series and scatter plots during calibration/validation at Jamshedpur, (e-h) Time-series and scatter plots during calibration/validation at Ghatshila

Since the model performance is reasonably good in simulating GW levels, it may augur well for obtaining the suitable values of geological parameters (Wijesekara et al. 2014).

Table 2 Performance evaluation measures for GWL simulation in different wells

		R ²	RMSE (m)	SD			R ²	RMSE (m)	SD
17,002	Calibration	0.89	0.70	1.53	16,991	Calibration	0.92	0.78	1.6
	Validation	0.55	1.2	1.7		Validation	0.70	0.91	2.0
16,977	Calibration	0.62	1.9	4.8	16,988	Calibration	0.76	1.4	3.1
	Validation	0.46	2.2	5.2		Validation	0.82	1.2	2.7
9736	Calibration	0.46	1.2	3.6	09,113	Calibration	0.71	1.45	3.1
	Validation	0.41	1.8	4.3		Validation	0.75	1.59	3.5

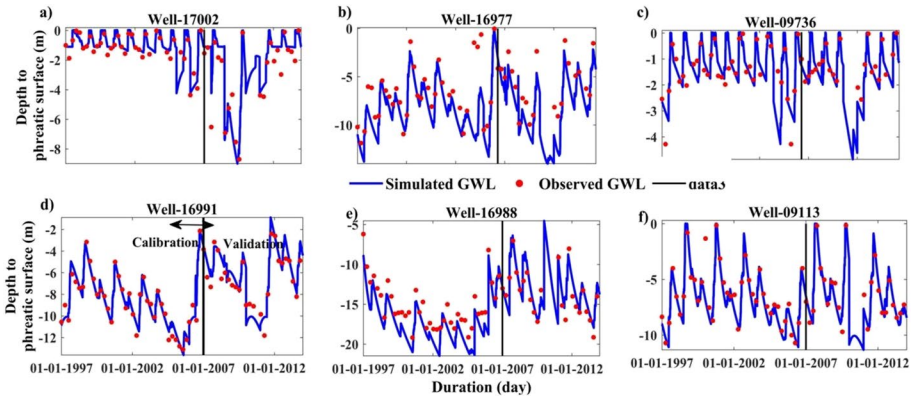


Fig. 4 Testing of hydrological model against GW levels: (a-f) Time series plot for calibration/validation at Well-17002, Well-16977, Well-09736, Well-16991, Well-16988, and Well-09113 respectively

3.2 Analysis of Uncertainties Due to Hydrological Impact Model

Figure 5(a) presents the daily 90% CI of streamflow during the calibration period at the Jamshedpur gauging station. Figure 5(b) presents the scatter plot between NQR and NQD

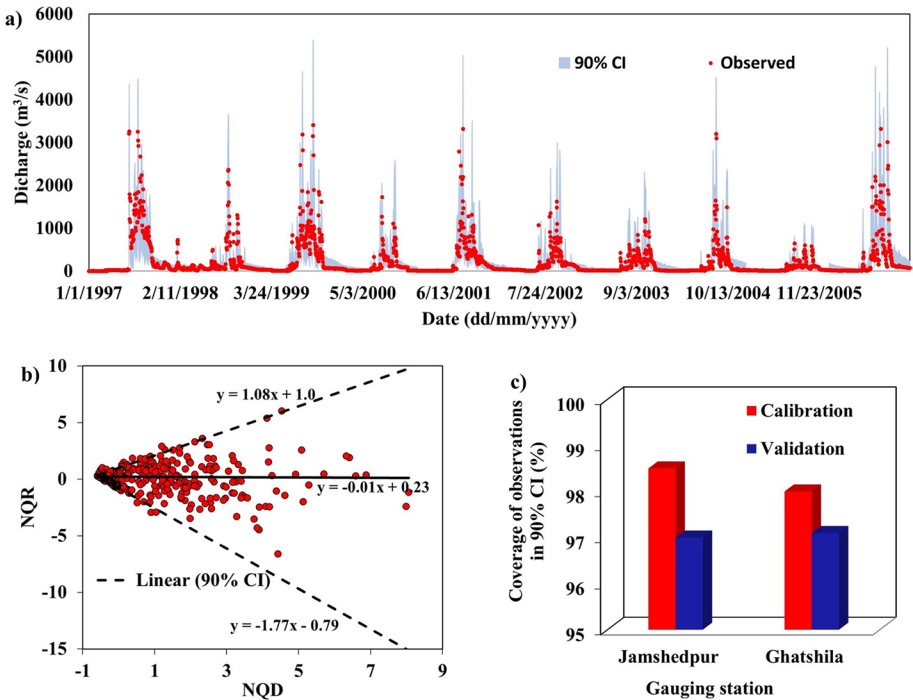


Fig. 5 a) Observed streamflow and uncertainty band along with error models of simulations in normalised domain during calibration period at Jamshedpur, b) scatter plot between NQR and NQD along with regression lines, c) coverage of observations in 90% CI during calibration and validation

along with three regression lines, i.e., the middle one corresponding to the median, and the rest two corresponding to the upper and lower limits of the 90% CI. The regression equation of each line presents the relationship between the residual and the simulated streamflow within the Gaussian domain. It is evident from Fig. 5(a) that most of the observed streamflow is bracketed by 90% CI; thus, endorsing the accuracy of the error model. Similarly, Fig. 5(b) confirms that the simulated streamflow is able to capture 95% of the observed streamflow during the calibration and validation periods. Figure 5(c) summarises the outcomes of QR by presenting the coverage of the observed data points in 90% CI during calibration/validation for two gauging stations. Figure 5(c) shows that 90% CI can capture more than 95% of the observed data points; thus, confirming the applicability of the error model. The per cent coverage of observed points in the uncertainty band (or the uncertainty band's width) shows that the uncertainty during the validation period is higher than that during the calibration period.

Figure 6(a) presents the daily 90% CI of GWL during the calibration period at Well 16,991 as an example. Figure 6(b) presents the scatter plot between NQR and NQD, along with three regression lines, described while presenting Fig. 6(b). It is evident from Fig. 6(a) that 90% CI can capture all observed points. Figure 6(c) presents the summary of QR for all Wells by presenting the coverage of 90% CI by observed points. Figure 6(c) suggests a good coverage of observed GWL points (> 85%) within the 90% CI band. The uncertainty, however, needs to be further analysed by incorporating more observed data points.

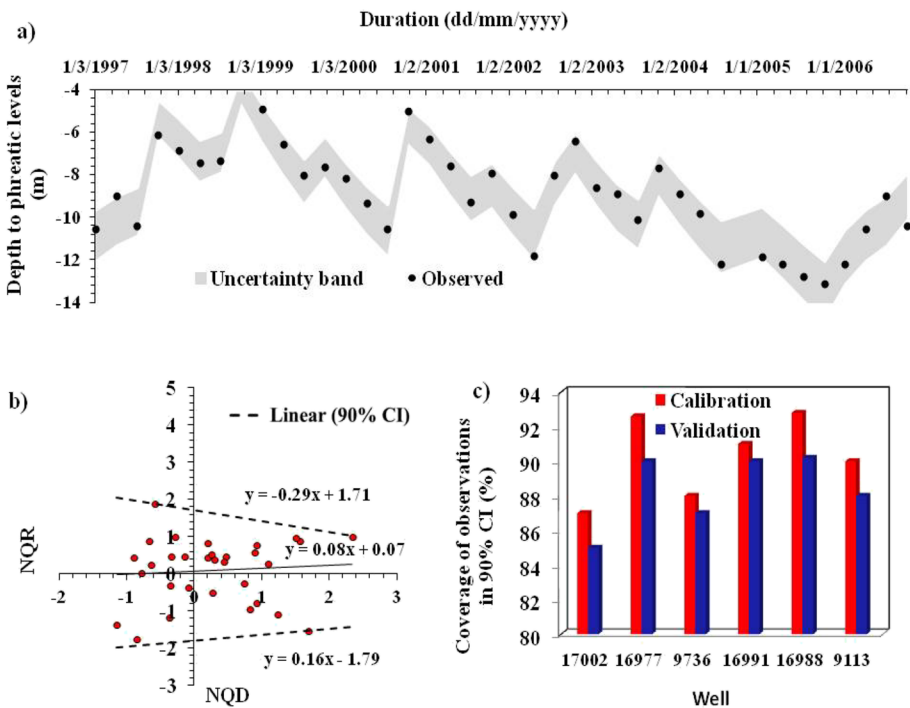


Fig. 6 a) Observed Groundwater levels and uncertainty band along with error models of simulations in normalized domain for calibration period at Well-16991, b) scatter plot between NQR and NQD with regression lines at Well-16991 during calibration period, c) Coverage of observations in 90% CI during calibration and validation of different wells

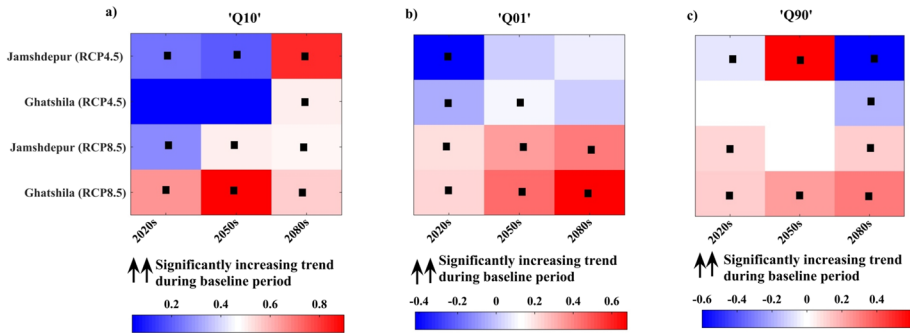


Fig. 7 Monotonic trends in **a)** Q₁₀ (high flows), **b)** Q₀₁ (very high flows), and **c)** Q₉₀ (low flows) during the 2020s, 2050s, and 2080s for RCP4.5 and RCP8.5 at Jamshedpur and Ghatshila stations. Black rectangle boxes at the center of the square indicate significant trend (at 5% significance level) based on MK test

3.3 Linkage Between the Combined LULC and Climate Change and Hydro-Climatic Extremes

3.3.1 Detection of Monotonic Trends of Hydrological Extremes in the Past and Future Records

Figure 7 presents the monotonic trends found using the MK test in Q₀₁, Q₁₀, and Q₉₀ during the 2020s, 2050s, and 2080s under RCP scenarios RCP4.5 and RCP8.5. For all extreme flows, significantly increasing trends were obtained during the baseline period. The shreds of evidence obtained from Fig. 7 are i) significantly increasing trends are found for 'Q₁₀' throughout the time-span except during the 2020s and 2050s (RCP4.5) at Ghatshila station. Non-significantly increasing trends are obtained during these exceptional periods. Overall, 'Q₁₀' trends are increasing (either significant or insignificant) at both stations. ii) 'Q₀₁' trends are found significantly increased for most of the time-periods, under RCP8.5; however, a mixture of significantly increasing and decreasing flows is found under RCP 4.5 at both stations. iii) 'Q₉₀' trends are found to be significantly increasing except during the 2050s (Jamshedpur (RCP8.5) and Ghatshila (RCP4.5) and 2020s (Ghatshila (RCP4.5)). Moreover, significantly decreasing trends are found during the 2080s for RCP4.5. Under RCP8.5, the overall 'Q₉₀' trends are found to be increasing. It is important to note that for 'Q₁₀' and 'Q₀₁', the trends appear to be more vital for the 2080s than the 2020s and 2050s.

Overall significant trends (either increasing or decreasing) could be attributed to ongoing and projected LULC changes, i.e., a decrease in dense forest and an increase in the basin's built-up area, as reported in Gaur et al. (2020b). The LULC trends possibly reduce the infiltration rate and result in increased runoff. The prominently increasing trends in Q₁₀ and Q₀₁ (mainly) could lead to increased flood hazards; however, increasing trends in Q₉₀ indicates a low risk of droughts in the Subarnarekha basin in future.

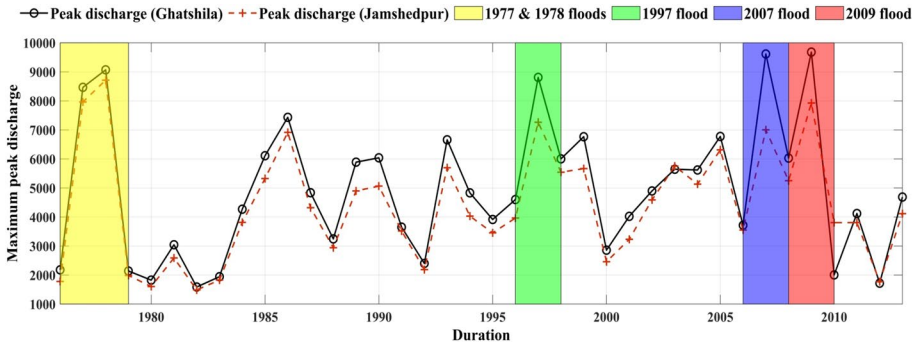


Fig. 8 Reconstruction of maximum peak discharge of major floods through hydrological impact model at Jamshedpur and Ghatshila stations. The coloured strips are showing the years during which flood occurred in the Subarnarekha basin

3.4 Ability of HM in Mimicking the Past Hydro-Climatic Behaviour

The ability of HM in mimicking the hydro-climatic behaviour of the basin is analysed in terms of maximum peak discharge (MPD). The year-wise MPD was extracted from the simulated MIKE SHE/MIKE HYDRO RIVER flow series. The observed flood records of the Subarnarekha basin was obtained from Singh and Giri (2018). The simulated MPD series can capture the significant floods observed in 1977, 1978, 1997, 2007, and 2009 during 1976–2015 at both gauging stations (Fig. 8). The coloured strips in Fig. 8 present the years during which the flood occurred in the Subarnarekha basin.

The results highlight the model’s credibility in regenerating the hydro-climatic behaviour of the Subarnarekha basin; thus, endorsing the model’s ability to project the future streamflows accurately.

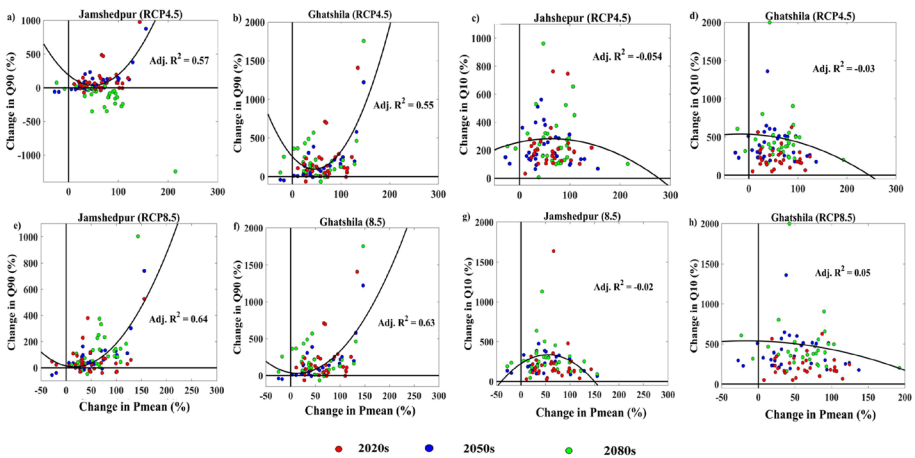


Fig. 9 Climate sensitivity under RCP4.5: **a)** Between Q_{90} and P_{mean} at Jamshedpur, **b)** Between Q_{90} and P_{mean} at Ghatshila, **c)** Between Q_{10} and P_{mean} at Jamshedpur, **d)** Between Q_{10} and P_{mean} at Ghatshila; climate sensitivity under RCP8.5: **e)** Between Q_{90} and P_{mean} at Jamshedpur, **f)** Between Q_{90} and P_{mean} at Ghatshila, **g)** Between Q_{10} and P_{mean} at Jamshedpur, **h)** Between Q_{10} and P_{mean} at Ghatshila. (Curve shows fitted local regression (polynomial) over all values, together with the adjusted R^2 values)

3.4.1 Evaluation of the Projected Effects of Climate Change on Future Extremes

Streamflow Climate Sensitivity Figure 9 illustrates the Q_{10} and Q_{01} anomalies against P_{mean} anomalies for the 2020s, 2050s, and 2080s. It is evident from Fig. 9 that streamflow is highly sensitive to precipitation and holds a nonlinear relationship. In the Subarnarekha basin, streamflow climate sensitivity is considerably high, i.e., small precipitation regime changes may cause enormous streamflow regime changes. An average 150% increase in annual precipitation causes a 600% increase in modelled annual discharge, whereas a 10% reduction in annual precipitation causes a 200% reduction in modelled annual discharge. However, in extreme cases, a 200% increase in annual precipitation causes a 2000% increase in modelled annual discharge, whereas a 25% reduction in annual precipitation causes a 350% reduction in modelled annual discharge. The range of variation is high for low flows than for high flows. The strength of the relationship is reasonably good for Q_{10} ($0.55 < Adj. R^2 < 0.64$), indicating the statistical significance of Q_{10} to P_{mean} trends. In low flows, the strength of the relationship is inferior ($R^2 < -0.05$), suggesting that Q_{90} to P_{mean} trend is not statistically significant. The uncertainties associated with RCMs, RCPs, and hydrological impact models appear to make this relationship, and hence, the consideration of uncertainty is essential (Pechlivanidis et al. 2017).

Our findings agree with Aich et al. (2014) and Kling et al. (2014), where authors have found high sensitivity of discharge to precipitation.

Analyses of Flow Duration Curves for Projected Flows Figure 10 presents the FDCs at Jamshedpur and Ghatshila stations under baseline, RCP4.5 and RCP8.5 scenarios. The projected FDC values show an increase in all flows (low, high, and medium) during the 2020s,

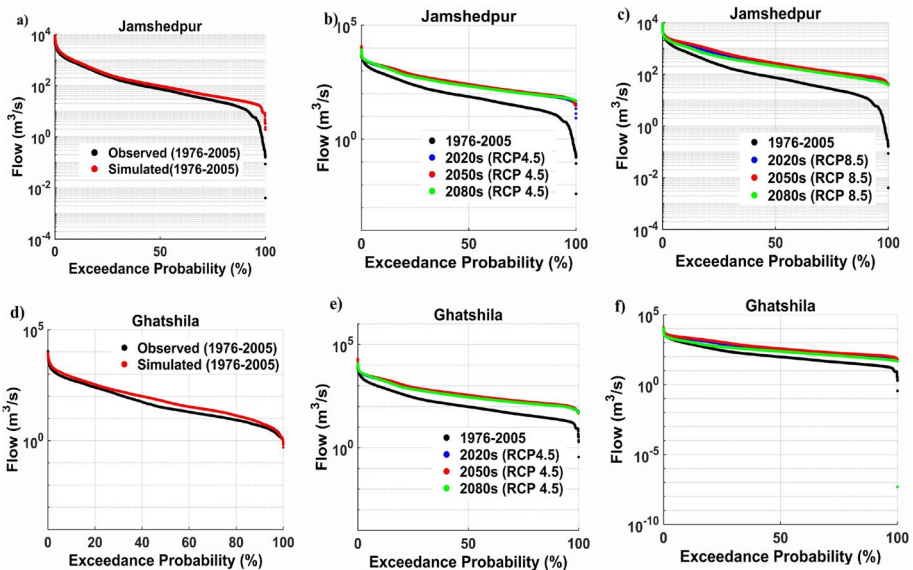


Fig. 10 Flow duration curves a) At Jamshedpur station during baseline period b) At Jamshedpur station under RCP4.5 scenario c) At Jamshedpur station under RCP8.5 scenario d) At Ghatshila station during baseline period e) At Ghatshila station under RCP4.5 scenario f) At Ghatshila station under RCP8.5 scenario

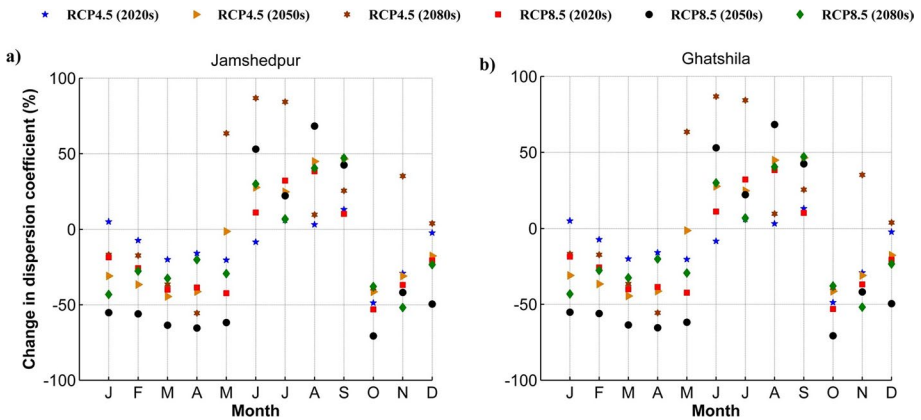


Fig. 11 Dispersion coefficient of projected streamflow compared to the baseline period at a) Jamshedpur b) Ghatshila

2050s, and the 2080s; however, the increase in low flows ($> Q_{80}$) is relatively high. Increasing high flows ($< Q_{20}$) suggests the susceptibility to flooding hazards in the basin. Changes in the climate and LULC could increase the basin's flows due to changing rainfall patterns, deforestation, and urbanisation. The FDC analysis shows that the low flows ($> Q_{80}$) would increase in the future; hence there would be a reduction in drought events during the 2020s, 2050s, and 2080s than in the baseline period.

Changes in Dispersion Coefficient Figure 11 presents the monthly per cent changes in the dispersion coefficient for streamflow in future periods relative to the baseline period. Ample decrease (5%-75%) in the monthly dispersion coefficient was projected for non-monsoon months (Jan-May and Oct-Dec), signifying more stable streamflow during these months under both RCPs. Conversely, a significant increase (5%-95%) is obtained during monsoon months (June-Sep) under both RCPs. Thus, the future streamflows could be highly

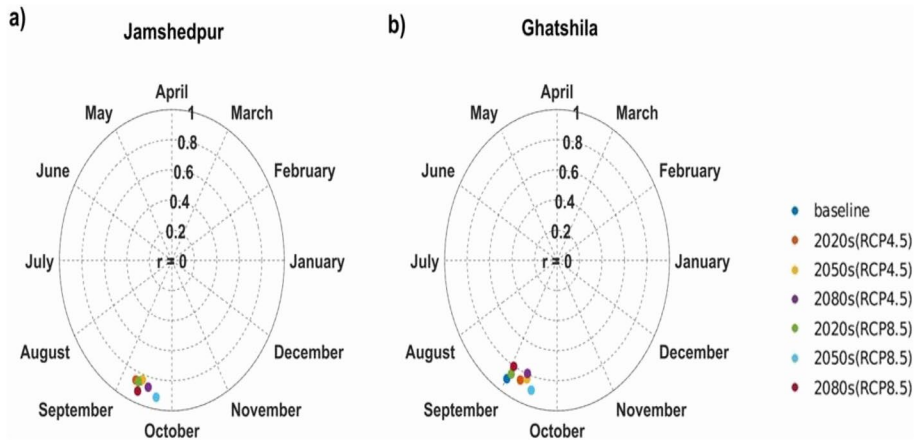


Fig. 12 The circular plots presenting mean date and persistence of the Peak Discharge Events (PDE) at a) Jamshedpur b) Ghatshila

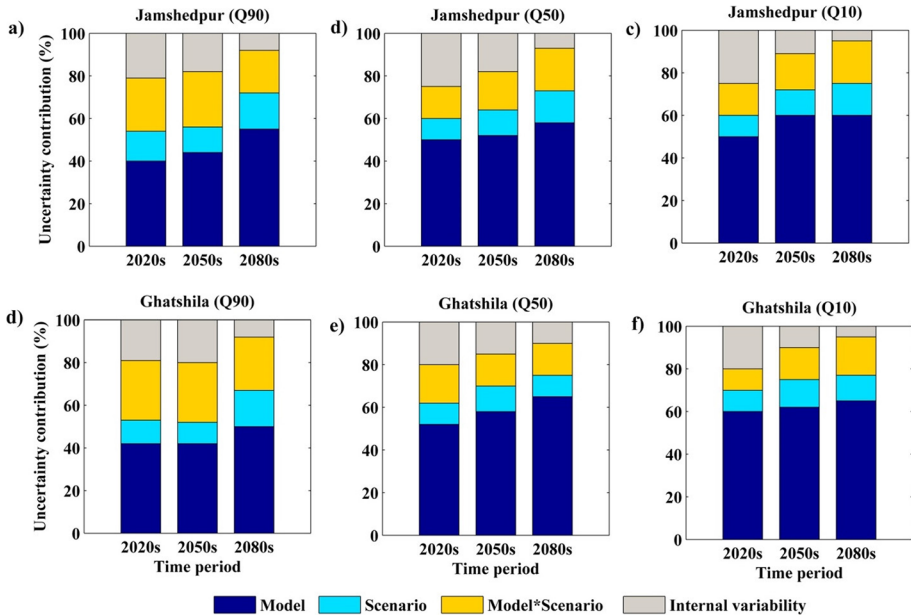


Fig. 13 Contribution of different factors to uncertainty of annual streamflow projections for **a)** Q₉₀ at Jamshedpur station **b)** Q₅₀ at Jamshedpur station **c)** Q₁₀ at Jamshedpur station **d)** Q₉₀ at Ghatshila station **e)** Q₅₀ at Ghatshila station **f)** Q₁₀ at Ghatshila station

unstable, with the likely occurrence of extreme events (i.e., floods in our case) during monsoon months. These findings are in agreement with the findings of Zhang et al. (2016).

Detection of the seasonality of PDE The seasonality measures of PDE are plotted as circular statistics to present the flood persistence and mean date of occurrence at Jamshedpur and Ghatshila stations (Fig. 12). The distance from the centre of the polar plot presents persistence, whereas the mean date of occurrence is denoted by measuring the counter-clockwise angle with respect to January 1. It is evident from Fig. 12 that the flood events are persistent across all periods, with mean flood dates concentrated around September. There appears to be a shift (delay) of around one to three weeks in the future periods' flood occurrence dates. Ghatshila station shows relatively more variation in the flood dates with varying persistence. Our findings corroborate the findings of Burn and Whitfield (2018) that there are a few (significant) changes in the flood seasonality.

3.5 Quantification of Uncertainty

Figures 13(a)-(f) present the segregation of different sources of uncertainty, i.e., RCMs, RCPs, the interaction between RCMs and RCPs, and internal variability in Q₁₀, Q₅₀, and Q₉₀. Figure 13(a)-(f) illustrates that the uncertainty stemming from RCMs dominates over the whole time-span (contributing to 40–62%), followed by uncertainty due to the interaction between RCMs and RCPs, internal variability, and RCPs. The dominance of uncertainty due to climate model has been warranted by numerous studies related to future climate projections, e.g., Bosshard et al. (2013);

Krysanova et al. (2017); Chawla and Mujumdar (2018) and Kim et al. (2019). The contribution of uncertainty due to RCM and RCP interaction also covers a significant proportion, implying the utility of consideration of interaction uncertainty for the future assessment of climate impacts on water resources, which agrees with Bosshard et al. (2013).

A closer look reveals that the fraction of uncertainty due to the internal variability decreased consistently from the 2020s to the 2080s. This decrease in the uncertainty due to the internal variability is in agreement with the IPCC (2013) report, which suggests the dominance of internal variability during the early-century. Next, RCP uncertainty also plays an important role; however, its contribution is relatively lower than that of other sources. Uncertainty due to RCPs signifies the consideration of different RCPs for the assessment of future climate change impacts.

4 Discussion

4.1 Utility of Integrated Modelling Systems

Unlike the previous study, i.e., Gaur et al. (2020a), the present study attempted to overcome the several limitations: i) distributed physically-based hydrological model is used instead of the conceptual model; ii) consideration of LULC changes have been taken into account; iii) uncertainty associated to model parameters, model structure, and model inputs are considered; iv) appropriate selection RCMs has been performed; v) prediction of hydro-climatic extremes has been performed under changing environmental conditions. The present study proposes an integrated modelling system that unites four comprehensive systems, i.e., spatially explicit LULC model, models to simulate the hydrological processes (i.e., flow model, MIKE SHE and river model MIKE HYDRO RIVER), and an ensemble of RCMs to simulate the hydro-climatology of the Subarnarekha basin. Moving a step forward from the previous studies that developed integrated modelling systems, i.e., Wijeskera (2013) and Farjad et al. (2017), we have integrated an ensemble of climate models along with the uncertainty framework in the existing framework. Development of the proposed integrated modelling system is crucial, as it offers the flexibility of changing the input dataset, parameters, and configuration with marginal modifications so that any application related to the sustainability of water resources can be easily added in future, e.g., to assess the variations in GW table as a consequence of LULC changes, or to examine the responses of altering streamflow to the future climate changes, and so on. Moreover, the integrated modelling system can also capture the underlying processes and nonlinear mechanisms of the system components and capture the interactions between land and water resources.

4.2 Methodologies for Understanding the Linkage Between Environmental Changes and Hydro-Climatic Extremes

The changing global environmental scenarios lend a new perspective to the climate and anthropogenic LULC changes on hydro-climatic extremes; however, for effective policy interventions, such investigations are equally required at a regional scale. Therefore, we have considered the linkages between the environmental changes and hydro-climatic

extremes for the Subarnarekha basin. LULC changes can significantly alter the hydrological cycle components by partitioning rainfall into components like runoff and evapotranspiration (Aduah et al. 2017). Climate change exaggerates the hydrological cycle components, with outcomes such as intensification in frequency and severity of droughts and floods. Besides, both these changes influence each other, e.g., LULC changes have feedbacks on regional climate through vegetation dynamics (Warburton et al. 2012). In other words, LULC change may have more effects on floods rather than droughts and normal flows in the watershed. The influence of LULC changes on the peak flow magnitudes may intensify when it shall occur in the same direction as the climate change impact.

Further, to unravel the linkage between such changes and hydro-climatic extremes, systematic methodologies need to be explored that deal with multiple aspects rather than focusing on a single aspect, such as identifying trends. Unlike the previous studies, e.g., Krysanova et al. (2017) and Pechlivanidis et al. (2017), we have analysed the changes in hydro-climatic extremes through more organised methodologies that deal with numerous aspects like sensitivity, occurrences, dispersion, and persistence. Such analysis will undoubtedly help design suitable adaptation and mitigation strategies interventions.

5 Conclusions

The present study evaluates the combined impact of climate and LULC changes on hydro-climatic extremes during the 2020s, 2050s, and 2080s for the Subarnarekha basin, a flood-prone river basin in Eastern India. Unlike the existing studies, we have attempted to understand better the climate and LULC changes through an integrated modelling system. The integrated modelling system is formed by combining a spatially explicit LULC model, a fully-distributed physically-based hydrological model, i.e., MIKE SHE/MIKE HYDRO RIVER and an ensemble of selected RCMs. In addition to this, we have also considered the uncertainties associated with different sources within the integrated modelling system. In this aspect, the selection of the hydrological impact model, i.e., a distributed physically-based MIKE SHE/MIKE HYDRO RIVER model compared to the lumped conceptual models, was the first step towards the uncertainty reduction. Various kinds of uncertainties associated with the hydrological impact model (i.e., parametric uncertainties, model input uncertainties, and model structure uncertainty) are studied through 'quantile regression.'

Further, the segregation of uncertainty due to different sources, i.e., RCMs, RCPs, RCM and RCP interaction, and internal variability, is performed through the 'ANOVA' approach. The key insights from the study and answer to the framed questions are as follows:

- For most future periods, significantly positive trends are obtained in extremes flows (Q_{10} , Q_{01} , and Q_{90}) except for a few periods at Jamshedpur and Ghatshila stations.
- The climate discharge sensitivity suggests that discharge is highly sensitive to precipitation in the Subarnarekha basin.
- A decrease of 5%-75% for non-monsoon months (Jan-May and Oct-Dec) and a significant increase of 5%-95% during monsoon months (June-Sep) is observed in the monthly dispersion coefficient.
- The future PDEs will probably be concentrated around the 'September' month with very low to no change in persistence.

- RCMs, followed by RCM and RCP interaction, are significant sources of uncertainty in the streamflow projections.

The LULC changes in the basin are responsible for alteration in peak flows, the medium flows, and low flows; furthermore, climate change is responsible for intensifying these flows. Overall findings suggest that the analysis and prediction of hydrological extremes under climate and LULC changes will be of great importance for preventing and mitigating hydrological disasters in the Subarnarekha basin. In the present study, the future LULC changes are assumed to follow the historical LULC growth pattern. Since LULC changes are dynamic, it may be interesting to incorporate and analyse the impact of various LULC scenarios reflecting the future development plans, e.g., the sustainable development plans, on the projected streamflows. We believe that the transferable methodological framework developed in this study could prove help understand the linkages between environmental changes and hydro-climatic extremes in various other basins around the world.

Supplementary Information The online version contains supplementary material available at <https://doi.org/10.1007/s11269-021-02817-3>.

Acknowledgement The World Climate Research Programme's Working Group on Regional Climate and the Working Group on Coupled Modelling, the former coordinating body of CORDEX and responsible panel for CMIP5, are gratefully acknowledged. The authors thank the Earth System Grid Federation (ESGF) infrastructure and the Climate Data Portal hosted at the Centre for Climate Change Research (CCCR), Indian Institute of Tropical Meteorology (IITM), for providing CORDEX South Asia data.

Authors Contributions Srishti Gaur: Conceptualisation, Data acquisition, Methodology, Writing- Original draft preparation. Arnab Bandyopadhyay: Supervision, Editing of the manuscript. Rajendra Singh: Conceptualisation, Supervision, Editing of the manuscript, Visualisation.

Availability of Data and Materials Data and material would be made available on request.

Declarations

Ethics Approval This article does not contain any studies with human participants or animals performed by any of the authors.

Conflict of Interest The author declares there is no conflict of interest.

References

- Aduah MS, Jewitt GPW, Toucher MLW (2017) Scenario-based impacts of land use and climate changes on the hydrology of a lowland rainforest catchment in Ghana, West Africa. *Hydrol Earth Syst Sci* 1–27. <https://doi.org/10.5194/hess-2017-591>
- Aich V, Liersch S, Vetter T (2014) Comparing impacts of climate change on streamflow in four large African river basins. *Hydrol Earth Syst Sci* 18:1305–1321
- Anaraki MV, Farzin S, Mousavi SF, Karami H (2021) Uncertainty Analysis of Climate Change Impacts on Flood Frequency by Using Hybrid Machine Learning Methods. *Water Resour Manag* 35:199–223
- Beven K, Feyen J (2002) The Future of Distributed Modelling. *Hydrol Process* 16:169–172
- Bosshard T, Carambia M, Goergen K et al (2013) Quantifying uncertainty sources in an ensemble of hydrological climate-impact projections. *Water Resour Res* 49:1523–1536
- Burn DH, Whitfield PH (2018) Changes in flood events inferred from centennial length streamflow data records. *Adv Water Resour* 121:333–349
- Chawla I, Mujumdar PP (2018) Partitioning uncertainty in streamflow projections under nonstationary model conditions. *Adv Water Resour* 112:266–282

- Dadson SJ, Lopez HP, Peng J, Vora S (2020) Hydroclimatic Extremes and Climate Change, In: Dadson SJ, Garrick DE, Penning-Rowsell EC, Hall JW, Hope R, Highes J. (Eds.), *Water Science, Policy, and Management: a Global Challenge*. John Wiley & Sons Ltd 11-28
- Farjad B, Gupta A, Razavi S, Faramarzi M, Marceau DJ (2017) An integrated modelling system to predict hydrological processes under climate and land-use/cover change scenarios. *Water* 9:1–23
- Gaur S, Bandyopadhyay A, Singh R (2020a) Modelling potential impact of climate change and uncertainty on streamflow projections: A case study. *J Water Clim Change*. <https://doi.org/10.2166/wcc.2020.254>
- Gaur S, Mittal A, Bandyopadhyay A et al (2020b) Spatio-temporal analysis of land use and land cover change: a systematic model inter-comparison driven by integrated modelling techniques. *Int J Remote Sens* 41:9229–9255
- Goyal MK, Surampalli RY (2018) Impact of climate change on water resources in India. *J Environ Eng Hamed KH, Ramachandra Rao A (1998) A modified Mann-Kendall trend test for autocorrelated data. J Hydrol* 204:182–196
- Hargreaves GH, Samani ZA (1985) Reference crop evapotranspiration from temperature. *Appl Eng Agric* 1: 96–99
- IPCC (2013) *Climate Change 2013: The Physical Science Basis*. Contribution of Working Group I to the Fifth Assessment Report of the Intergovernmental Panel on Climate Change. Cambridge University Press, Cambridge, United Kingdom and New York, NY, USA, 1535
- Kendall MG (1975) *Rank Correlation method*, 4th edn. Charles Griffen, London
- Kim Y, Ohn I, Lee JK, Kim YO (2019) Generalizing uncertainty decomposition theory in climate change impact assessments. *J Hydrol X* 3:100024
- Kim S, Alizamir M, Kim NW, Kisi O (2020) Bayesian model averaging: A unique model enhancing forecasting accuracy for daily streamflow based on different antecedent time series. *Sustain* 12:1–22
- Kling H, Stanzel P, Preishuber M (2014) Impact modelling of water resources development and climate scenarios on Zambezi River discharge. *J Hydrol Reg Stud* 1:17–43
- Krysanova V, Vetter T, Eisner S et al (2017) Intercomparison of regional-scale hydrological models and climate change impacts projected for 12 large river basins worldwide - A synthesis. *Environ Res Lett* 12. <https://doi.org/10.1088/1748-9326/aa8359>
- Kumar A, Singh R, Jena PP et al (2015) Identification of the best multi-model combination for simulating river discharge. *J Hydrol* 525:313–325
- Kundzewicz ZW, Krysanova V, Benestad RE et al (2018) Uncertainty in climate change impacts on water resources. *Environ Sci Policy* 79:1–8
- Laaha G, Blöschl G (2006) Seasonality indices for regionalising low flows. *Hydrol Process* 20:3851–3878
- Lee JK, Kim YO, Kim Y (2017) A new uncertainty analysis in the climate change impact assessment. *Int J Remote Sens* 37(10):3837–3846
- Mann HB (1945) Nonparametric tests against trend. *Econometrica* 13:245–259
- Mohammadi B, Ahmadi F, Mehdizadeh S et al (2020a) Developing Novel Robust Models to Improve the Accuracy of Daily Streamflow Modeling. *Water Resour Manag* 34:3387–3409
- Mohammadi B, Linh NTT, Pham QB et al (2020b) Adaptive neuro-fuzzy inference system coupled with shuffled frog leaping algorithm for predicting river streamflow time series. *Hydrol Sci J* 65:1738–1751
- Moriasi DN, Arnold JG, Van Liew MW et al (2007) Model Evaluation Guidelines for Systematic Quantification of Accuracy in Watershed Simulations. *Trans ASABE* 50:885–900
- Norouzi Khatiri K, Niksokhan MH, Sarang A, Kamali A (2020) Coupled Simulation-Optimization Model for the Management of Groundwater Resources by Considering Uncertainty and Conflict Resolution. *Water Resour Manag* 34:3585–3608
- Paul PK, Gaur S, Kumari B et al (2019) Diagnosing Credibility of a Large-Scale Conceptual Hydrological Model in Simulating Streamflow. *J Hydrol Eng* 24:04019004. [https://doi.org/10.1061/\(asce\)he.1943-5584.0001766](https://doi.org/10.1061/(asce)he.1943-5584.0001766)
- Pechlivanidi IG, Arheimer B, Donnelly C (2017). Analysis of hydrological extremes at different hydro-climatic regimes under present and future conditions. *Clim Change*, 467–481. <https://doi.org/10.1007/s10584-016-1723-0>
- Piani C, Haerter JO, Coppola E (2010) Statistical bias correction for daily precipitation in regional climate models over Europe. *Theor Appl Climatol* 187–192. <https://doi.org/10.1007/s00704-009-0134-9>
- Sen PK (1968) Estimates of the Regression Coefficient Based on Kendall's Tau. *J Am Stat Asso* 63 (324)

- Serneels S, Said MY, Lambin EF (2001) Land cover changes around a major East African wildlife reserve: The Mara ecosystem (Kenya). *Int J Remote Sens.* 22(17):3397–3420
- Singh AK, Giri S (2018) Subarnarekha River: The Golden Streak of India, In: Singh, D.S. (Ed.). *The Indian Rivers*. Springer, Singapore. <https://doi.org/10.1007/978-981-10-2984-4>
- Singh R (2019) Stochastic modelling for the spatio-temporal analysis of rainfall patterns Dissertation. Indian Institute of Technology, Kharagpur
- Storch H, Von, Geesthacht H, Navarra A (1999) *Analysis of climate variability*. Springer-Verlag Berlin Heidelberg. <https://doi.org/10.1007/978-3-662-03744-7>
- Tabari MMR (2015) *Conjunctive Use Management under Uncertainty Conditions in Aquifer Parameters*. *Water Resour Manag* 29:2967–2986
- Warburton ML, Schulze RE, Jewitt GPW (2012) Hydrological impacts of land use change in three diverse South African catchments. *J Hydrol* 414–415:118–135
- Weerts AH, Winsemius HC, VerkadeBox JS (2011) Estimation of predictive hydrological uncertainty using quantile regression : examples from the National Flood Forecasting System (England and Wales). *Hydrol Earth Syst Sci.* 15:255–265
- Wijesekara G (2013) *An integrated modeling system to simulate the impact of land-use changes on hydrological processes in the Elbow River watershed in Southern Alberta*. Dissertation, University of Alberta
- Wijesekara GN, Gupta A, Valeo C et al (2012) Assessing the impact of future land-use changes on hydrological processes in the Elbow River watershed in southern Alberta, Canada. *J. Hydrol* 412–413:220–232
- Wijesekara GN, Farjad B, Gupta A et al (2014) A comprehensive land-use/hydrological modeling system for scenario simulations in the Elbow River watershed, Alberta, Canada. *Environ Manage* 53:357–381
- Zhang Y, You Q, Chen C, Ge J (2016) Impacts of climate change on streamflows under RCP scenarios: A case study in Xin River Basin, China. *Atmos Res* 178–179:521–534

Publisher's Note Springer Nature remains neutral with regard to jurisdictional claims in published maps and institutional affiliations.

Authors and Affiliations

Srishti Gaur¹  · Arnab Bandyopadhyay²  · Rajendra Singh¹

Arnab Bandyopadhyay
arnabbandy@yahoo.co.in

Rajendra Singh
rsingh@agfe.iitkgp.ac.in

¹ Agricultural and Food Engineering, Indian Institute of Technology, West Bengal 721302 Kharagpur, India

² Department of Agricultural Engineering, North Eastern Regional Institute of Science and Technology, Arunachal Pradesh 791109 Nirjuli (Itanagar), India